Atmospheric Chemistry and Physics

Laboratory study on new particle formation from the reaction OH + SO$_2$: influence of experimental conditions, H$_2$O vapour, NH$_3$ and the amine tert-butylamine on the overall process

T. Berndt[1], F. Stratmann[1], M. Sipilä[1,2,*], J. Vanhanen[2], T. Petäjä[2], J. Mikkilä[2], A. Grüner[1], G. Spindler[1], R. Lee Mauldin III[3], J. Curtius[4], M. Kulmala[2], and J. Heintzenberg[1]

[1]Leibniz-Institut für Troposphärenforschung e.V., Permoserstr. 15, 04318 Leipzig, Germany
[2]Department of Physics, University of Helsinki, P.O. Box 64, 00014, Finland
[3]Atmospheric Chemistry Division, Earth and Sun Systems Laboratory, National Center for Atmospheric Research,
P.O. Box 3000, Boulder, CO 80307-5000, USA
[4]Institute for Atmospheric and Environmental Sciences, Goethe-University Frankfurt am Main,
60438 Frankfurt am Main, Germany
*also at: Helsinki Institute of Physics, University of Helsinki, P.O. Box 64, 00014, Finland

Abstract. Nucleation experiments starting from the reaction of OH radicals with SO$_2$ have been performed in the *IfT-LFT* flow tube under atmospheric conditions at 293±0.5 K for a relative humidity of 13–61%. The presence of different additives (H$_2$, CO, 1,3,5-trimethylbenzene) for adjusting the OH radical concentration and resulting OH levels in the range (4–300) ×10^5 molecule cm^{-3} did not influence the nucleation process itself. The number of detected particles as well as the threshold H$_2$SO$_4$ concentration needed for nucleation was found to be strongly dependent on the counting efficiency of the used counting devices. High-sensitivity particle counters allowed the measurement of freshly nucleated particles with diameters down to about 1.5 nm. A parameterization of the experimental data was developed using power law equations for H$_2$SO$_4$ and H$_2$O vapour. The exponent for H$_2$SO$_4$ from different measurement series was in the range of 1.7–2.1 being in good agreement with those arising from analysis of nucleation events in the atmosphere. For increasing relative humidity, an increase of the particle number was observed. The exponent for H$_2$O vapour was found to be 3.1 representing an upper limit. Addition of 1.2×10^{11} molecule cm^{-3} or 1.2×10^{12} molecule cm^{-3} of NH$_3$ (range of atmospheric NH$_3$ peak concentrations) revealed that NH$_3$ has a measureable, promoting effect on the nucleation rate under these conditions. The promoting effect was found to be more pronounced for relatively dry conditions, i.e. a rise of the particle number by 1–2 orders of magnitude at RH = 13% and only by a factor of 2–5 at RH = 47% (NH$_3$ addition: 1.2×10^{12} molecule cm^{-3}). Using the amine tert-butylamine instead of NH$_3$, the enhancing impact of the base for nucleation and particle growth appears to be stronger. Tert-butylamine addition of about 10^{10} molecule cm^{-3} at RH = 13% enhances particle formation by about two orders of magnitude, while for NH$_3$ only a small or negligible effect on nucleation in this range of concentration appeared. This suggests that amines can strongly influence atmospheric H$_2$SO$_4$-H$_2$O nucleation and are probably promising candidates for explaining existing discrepancies between theory and observations.

1 Introduction

Simultaneous measurements of newly formed ultra-fine particles and H$_2$SO$_4$ in the lower troposphere reveal that new particle formation is strongly connected to the occurrence of H$_2$SO$_4$ with concentrations of about 10^5–10^7 molecule cm^{-3} (Weber et al., 1996, Sihto et al., 2006, Riipinen et al., 2007). As a result of these studies kinetic analysis shows that the production rate of new particles can be described by a power law equation for H$_2$SO$_4$ with an exponent in the range of 1–2. From a mechanistic point of view, an exponent of 1 for H$_2$SO$_4$ can be explained by activation of pre-existing clusters

by H$_2$SO$_4$, and an exponent of 2 by a simple bimolecular step for H$_2$SO$_4$ being rate limiting in the course of nucleation (McMurry and Friedlander, 1979, Kulmala et al., 2006, Sihto et al., 2006, Riipinen et al., 2007). For the bimolecular step, this finding suggests that the critical cluster consists of 2 H$_2$SO$_4$ molecules. The range of H$_2$SO$_4$ concentration observed for nucleation events in both laboratory and field as well as the deduced H$_2$SO$_4$ cluster composition are in contradiction to the predictions of classical binary nucleation theory for H$_2$SO$_4$/H$_2$O (Kulmala et al., 1998).

Recently, the re-analysis of existing data sets from different measurement sites by Kuang et al. (2008) yielded an exponent of 2 within a very small range of uncertainty. This finding favours a bimolecular reaction of H$_2$SO$_4$ producing the critical cluster. The deduced rate coefficient for this step shows variation by three orders of magnitude. For explanation, Kuang et al. (2008) propose the existence of a further gas-phase species that co-nucleates with H$_2$SO$_4$ and stabilises the critical cluster.

From laboratory measurements a relatively wide range for the number of H$_2$SO$_4$ molecules in the critical cluster (slope: $\Delta\log(J)/\Delta\log([\mathrm{H_2SO_4}])$) as well as for the threshold H$_2$SO$_4$ concentration needed for nucleation is reported. For experiments using H$_2$SO$_4$ from a liquid source, nucleation for different relative humidities was detectable for concentrations above 10^9–10^{10} molecule cm^{-3} (Wyslouzil et al., 1991; Viisanen et al., 1997; Ball et al., 1999; Zhang et al., 2004). It was concluded from particle number measurements as a function of H$_2$SO$_4$ concentration that 4–30 molecules of H$_2$SO$_4$ are present in the critical cluster.

Experiments starting from the reaction of OH radicals with SO$_2$ for in-situ H$_2$SO$_4$ formation by Young et al. (2008) yielded threshold H$_2$SO$_4$ concentrations needed for nucleation of 10^8–10^9 molecule cm^{-3}. From measured slopes $\Delta\log(J)/\Delta\log([\mathrm{H_2SO_4}])$ the researchers concluded that the critical cluster contains 3–8 H$_2$SO$_4$ molecules.

From our laboratory, however, using also the reaction of OH radicals with SO$_2$ for H$_2$SO$_4$ formation (Berndt et al., 2005), experimental evidence for the formation of new particles was found for H$_2$SO$_4$ concentrations of $\sim$10^7 molecule cm^{-3}. The analysis of integral number measurements by means of commercially available UCPCs (UCPC: Ultrafine Condensation Particle Counter) revealed that measured slopes of log(N) vs. log([H$_2$SO$_4$]) were affected by the decreasing size-dependent counting efficiency of the UCPCs used for $dp<3$ nm leading to an overestimation of the slope log(N) vs. log([H$_2$SO$_4$]). Therefore, any discussions regarding the composition of the critical cluster have been omitted so far (Berndt et al., 2005).

Recently, in two papers (Berndt et al., 2008, Laaksonen et al., 2008) the old idea dating from the eighties was discussed that HSO$_5$ as an intermediate from OH initiated SO$_2$ oxidation could trigger new particle formation (Friend et al., 1980). The experimental finding that high NO concentrations can suppress nucleation was taken as an argu-

ment supporting the potential role of HSO$_5$ (Friend et al., 1980; Berndt et al., 2008; Laaksonen et al., 2008). Very recently, Sipilä et al. (2010) showed experimentally that with the help of high efficiency particle counters (Sipilä et al., 2009; Vanhanen, 2009) new particle formation can be observed in the laboratory for H$_2$SO$_4$ concentrations down to $\sim$10^6 molecule cm^{-3}. As a result of this study, there exists no clear discrepancy in the results of nucleation experiments using either H$_2$SO$_4$ from a liquid reservoir or producing H$_2$SO$_4$ in situ via the reaction of OH radicals with SO$_2$. From the viewpoint of process engineering the critical issues in comparing the different experiments are the different H$_2$SO$_4$ profiles in the flow tubes (point source of H$_2$SO$_4$ or continuous H$_2$SO$_4$ production) in connection with significant wall losses, and the efficiency of the activation and growth process inside the particle counters used, cf. Sipilä et al. (2010). These findings relativise the possible role of HSO$_5$ products in the nucleation process. However, it remains unclear what the reason for the observed NO effect on nucleation rate is (Berndt et al., 2008).

The primary aim of this work is to investigate the possible role of H$_2$O vapour and NH$_3$ for new particle formation using high efficiency particle counters (detection limit of $\sim$1.5 nm mobility diameter) as well as DMPS measurements for investigations at relatively high H$_2$SO$_4$ concentrations (relatively high particle numbers with large diameter). NH$_3$ is believed to represent a third body in the atmospheric nucleation process and theoretical studies proposed that atmospheric mixing ratios of NH$_3$ at pptv-level can stabilize the critical cluster (Coffman and Hegg, 1995, Korhonen et al., 1999). This idea has been supported by Ball et al. (1999) showing experimentally that tens of pptv of NH$_3$ enhances considerably the nucleation rate at a relative humidity of $\sim$5 or 15% and for H$_2$SO$_4$ concentrations in the nucleation zone of $>5\times10^{10}$ molecule cm^{-3}. More recently, a re-evaluation at theoretical level shows that even a mixing ratio of 1–10 ppbv NH$_3$ is not able to trigger nucleation at 295 K unless the H$_2$SO$_4$ concentration accounts for at least 10^9 molecule cm^{-3} (Anttila et al., 2005; Merikanto et al., 2007). Benson et al. (2009) published experimental data for a temperature of 288 K showing an up to thousand-fold increase of the nucleation rate in the case of added NH$_3$ at levels of 10–50 ppbv under conditions of 10^8–10^9 molecule cm^{-3} of H$_2$SO$_4$ in the system. The nucleation-enhancing effect by NH$_3$ increased with decreasing H$_2$SO$_4$ concentrations and decreasing relative humidity. Hanson and Eisele (2002) describe measurements of clusters consisting of H$_2$SO$_4$ and NH$_3$. At 285 K and for H$_2$SO$_4$ and NH$_3$ concentrations of 1.9×10^9 and 3.5×10^9 molecule cm^{-3}, respectively, several 10^5 cluster cm^{-3} were detected. Generally, NH$_3$ containing clusters were found being more stable than H$_2$SO$_4$ clusters in absence of NH$_3$. A critical cluster composition of 2 H$_2$SO$_4$ molecules and 1 NH$_3$ molecule is favoured.

Kurten et al. (2008) performed a comparative study regarding the role of NH$_3$ and a series of amines in the atmospheric nucleation process by means of quantum chemical methods. It was concluded that amines can more efficiently support the nucleation than NH$_3$ as the estimated 2–3 order of magnitude lower amine concentrations in atmosphere are overcompensated by the amine-H$_2$SO$_4$ complexes being much stronger bonded.

In a case study, using tert-butylamine as an example, also first experimental results regarding the role of amines for nucleation are presented here.

2 Experimental

The nucleation experiments have been carried out in the atmospheric pressure flow-tube *IfT*-LFT (i.d. 8 cm; length 505 cm) at 293±0.5 K (Berndt et al., 2005). The flow tube consists of a first section (56 cm) that includes the inlet system for gas input (humidified air premixed with SO$_2$ from a calibration gas mixture, O$_3$ from an ozone generator outside of the flow tube and the OH scavengers H$_2$, CO or 1,3,5-trimethylbenzene). The second section with a length of 344 cm (middle section) is equipped with 8 UV lamps (Hg-lamps made of quartz-glass PN235 with a cut-off wavelength of 210 nm) for a homogeneous irradiation of the tube. At the end of a third, non-irradiated section (105 cm) the sampling outlets are attached.

Relative humidity was measured by means of a humidity sensor (Vaisala), O$_3$ and SO$_2$ by means of gas monitors (Thermo Environmental Instruments: 49C and 43C) or by long-path UV absorption spectroscopy (Perkin-Elmer: Lambda 800) using a gas cell with a White-mirror optics adjusted at a path-length of 512 cm.

As the carrier gas served high-purity synthetic air (99.9999999%, Linde and further purification with GateKeeper CE-500KF-O-4R, AERONEX). Stated output gas impurity from GateKeeper is <500 ppt ($\sim$1.2×10^{10} molecule cm^{-3}) for NMHCs, H$_2$O and CO$_2$ in sum. The NH$_3$ concentration in the carrier gas was found to be below the stated detection limit of 2.5×10^9 molecule cm^{-3} measured by means of a trace gas monitor TGA 310 (OMNISENS). The performance of TGA 310 was checked using a NIST NH$_3$ standard (type 40F3). Simultaneously, NH$_3$ concentrations were measured by long-path UV absorption confirming the certification of the standard. There were no indications that TGA 310 was not functioning properly.

O$_3$ was produced outside of the flow tube by passing a small fraction of the carrier gas through an ozone generator (UVP OG-2). SO$_2$ was taken from a 1 ppmv or 10 ppmv calibration mixture in N$_2$ (Messer). The water needed for the gas humidifier was obtained from an ultrapure water system (Barnstead, resistivity: 17.4 MΩ cm). CO (99.997%, Air Liquide), 1,3,5-trimethylbenzene (99%, Fluka), NH$_3$

(Merck, >99.9%) and tert-butylamine (Fluka, >99.5%) diluted with a carrier gas were supplied by a gas metering unit. H$_2$ (99.999%, Messer) was directly added to the carrier gas flow. On-line GC-FID connected with a cryo-enrichment device (detection limit for organics: a few 10^9 molecule cm^{-3} depending on the chemical structure) was applied for measuring the consumption of 1,3,5-trimethylbenzene. Initial reactant concentrations were (unit: molecule cm^{-3}); O$_3$: (3.6–4.4)×10^{11}; SO$_2$: (0.21 - 104)×10^{10}; CO: 2.1×10^{14}; 1,3,5-trimethylbenzene: 8.4×10^{11}; H$_2$: (1.77–240)×10^{15}. The conversion of O$_3$ covered the range of 3.1–42%.

The total gas flow inside the *IfT*-LFT was set at 3.33, 10, 11, 20, 30, 40, or 50 l min^{-1} STP resulting in a bulk residence time in the irradiated middle sections of 290, 97, 88, 48, 32, 24, or 19.3 s, respectively. The corresponding bulk residence times for middle and end section are 378, 126, 115, 62, 42, 34, or 25.2 s, respectively. All gas flows were set by means of calibrated gas flow controllers (MKS 1259/1179) and the pressure in the tube was measured using a capacitive manometer (Baratron). If the gas flow required for the analyzers was higher than the carrier flow, the analyzers were connected to the flow tube individually. No dilution techniques were applied. CI-MS measurements were possible only for a total flow of 11 l min^{-1} or higher.

For integral particle measurements a butanol-based UCPC (TSI 3025) as well as a H$_2$O-based UCPC (TSI 3786) have been applied. Measuring particle size distributions, a differential mobility particle sizer (DMPS) consisting of a Vienna-type DMA and a butanol-based UCPC (TSI 3025) were used. For retrieving the size information from the measured mobility distributions, an inversion algorithm according to Stratmann and Wiedensohler (1996) was applied. Besides the bipolar equilibrium charge distribution, in the inversion algorithm, experimentally determined DMA transfer functions and CPC counting efficiencies, and particle losses in the sampling lines are accounted for.

2.1 High sensitivity particle measurements

A pulse height analysing ultrafine condensation particle counter, PHA-UCPC, (Weber et al., 1995) as well as a mixing-type CPC, M-CPC (Vanhanen, 2009), came into operation allowing the detection of particles with a diameter down to about 1.5 nm. The PHA-UCPC comprises a butanol-based UCPC (TSI 3025A) with modified white light optics and a multi-channel analyser (Dick et al., 2000). Pulse height analysis technique allows distinguishing between homogeneously nucleated droplets and droplets formed by heterogeneous nucleation on particles with sizes below 2 nm in mobility diameter (Sipilä et al., 2008, 2009). Therefore, very high butanol super-saturations can be used to maximize the detection efficiency at sub-3 nm size range. The saturator temperature of the UCPC was increased from nominal 37°C up to 43°C. Condenser temperature was kept at 10°C. Solving heat and mass transfer equations yielded the maximum saturation

ratio of $S \approx 4.0$ (in nominal operation settings $S \approx 3.1$). The detection efficiency – MCA channel relation of the PHA-UCPC was calibrated using ammonium sulphate particles classified in a high resolution DMA. Since the pulse height response is sensitive to particle chemical composition, the particle diameter – MCA channel relation was corrected using sulphuric acid particles produced in *IfT*-LFT and classified with a very short (11 mm) Vienna-type DMA (Sipilä et al., 2010). A detailed description of the modified PHA-UCPC and its calibration as well as data inversion procedures are given in Sipilä et al. (2009).

The M-CPC comprises a particle size magnifier, PSM (Vanhanen et al., 2009), and an external CPC (TSI-3010). PSM is used to activate and grow sub 2 nm particles to sizes detectable with a simple CPC. Design of the PSM bases on the work of Sgro and Fernández de la Mora (2004). As the working fluid, diethylene glygol is used. Choice of the working fluid bases on the findings by Iida et al. (2009) who concluded that due to its high surface tension and low saturation vapour pressure a high saturation ratio is acquired without homogeneous nucleation. Thus, the activation of existing seed aerosol down to sizes well below 2 nm becomes possible in absence of background from homogeneous nucleation. Calibration results (Vanhanen et al., 2009) have shown that PSM detects charged particles with unity approaching efficiency (practically diffusion loss limited) down to ∼1.5 nm. Below that still >50% of the smallest calibration ion, tetramethyl-ammonium-ion, with mobility equivalent diameter of 1.05 nm, was activated in the PSM in comparison to reference electrometer. Since the particle sizes in our experiments ranged up from ∼1.3 nm, we assume the unity detection efficiency for the M-CPC in this study.

2.2 CI-MS measurements

Sulfuric acid in the *IfT*-LFT was measured with a Chemical Ionization Mass spectrometer, CI-MS (Eisele and Tanner, 1993; Mauldin et al., 1998; Petäjä et al., 2009). In short, the measurement proceeds as follows. The sulfuric acid in the sample flow is chemically ionized by (NO$_3^-$) ions. The reagent ions are generated by nitric acid and a ^{241}Am alpha source and mixed in a controlled manner in a drift tube utilizing concentric sheath and sample flows together with electrostatic lenses.
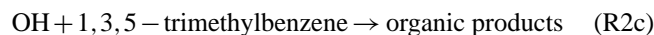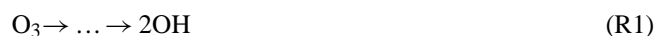
Prior to entering the vacuum system, the chemically ionized sulfuric acid molecules pass through a layer of dry nitrogen flow in order to dehydrate the sulfuric acid. In the vacuum system the sulfuric acid clusters are dissociated to the core ions by collisions with the nitrogen gas seeping through the pinhole in the collision-dissociation chamber (Eisele and Tanner, 1993). The sample beam is collimated with a set of conical octopoles, mass filtered with a quadrupole and detected with a channeltron. The sulfuric acid concentration is determined by the ratio between the signals at mass 97 amu (HSO$_4^-$) and the reagent ion at mass 62 amu (NO$_3^-$) multi-

plied by the instrument and setup dependent calibration factor.

The calibration factor is determined by photolyzing ambient water vapor with a mercury lamp to generate a known amount of OH radicals in front of the inlet (e.g. Mauldin et al., 2001). The produced OH radicals subsequently convert isotopically labeled ^{34}SO$_2$ into labeled sulfuric acid in a well defined reaction time yielding finally after ionization (H^{34}SO$_4^-$). A nominal detection limit of the CI-MS instrument is 5×10^4 molecule cm^{-3} for a 5 min integration period.

2.3 Determination of H$_2$SO$_4$ concentration

Besides CIMS, H$_2$SO$_4$ concentrations were also determined using model calculations according to the following reaction scheme (Berndt et al., 2005):

$$O_3 \rightarrow \ldots \rightarrow 2OH \quad \text{(R1)}$$

$$OH + H_2 \rightarrow products \quad \text{(R2a)}$$

$$OH + CO \rightarrow products \quad \text{(R2b)}$$

$$OH + 1,3,5 - trimethylbenzene \rightarrow organic\ products \quad \text{(R2c)}$$

$$OH + SO_2 \rightarrow \ldots \rightarrow H_2SO_4 \quad \text{(R3)}$$

$$H_2SO_4 \rightarrow wall \quad \text{(R4)}$$

For each experiment the effective photolysis rate coefficient k_1 was determined separately measuring the O$_3$ decay. A very stable photolysis rate was found during the whole measurement period confirming stable operation conditions of the UV lamps. In order to adjust the needed OH radical level in the flow tube, either H$_2$, CO or 1,3,5-trimethylbenzene were added consuming the major fraction of generated OH radicals. Rate coefficients (unit: cm^3 molecule^{-1} s^{-1}) $k_{R2a} = 6.7 \times 10^{-15}$, $k_{R2b} = 2.4 \times 10^{-13}$ (DeMore et al., 1997), $k_{R2c} = 5.7 \times 10^{-11}$ (Kramp and Paulson, 1998) and $k_{R3} = 1.2 \times 10^{-12}$ (Zellner, 1978) were taken from literature. From results given by Stockwell and Calvert (1983) it can be concluded that more than 80% of the reacted SO$_2$ is converted to H$_2$SO$_4$. Therefore, the assumption of a formation yield of unity for H$_2$SO$_4$ from the overall process of SO$_2$ oxidation (pathway R3) should be applicable. For the wall loss of H$_2$SO$_4$, a diffusion controlled process is assumed applying $k_{R4} = 3.65 \cdot D(H_2SO_4)/r^2$ with the diffusion coefficient $D(H_2SO_4)$ given by Hanson and Eisele (2000). The stated H$_2$SO$_4$ concentrations represent average values for the irradiated middle section.

In Fig. 1 examples of H$_2$SO$_4$ profiles in the irradiated middle section and the end section of the *IfT*-LFT are given for SO$_2$ concentrations of 6.3×10^9 and 5.3×10^{10} molecule cm^{-3} (total flow: 111 min^{-1} STP; O$_3$: 3.5×10^{11} molecule cm^{-3}; CO: 2.1×10^{14} molecule cm^{-3}).
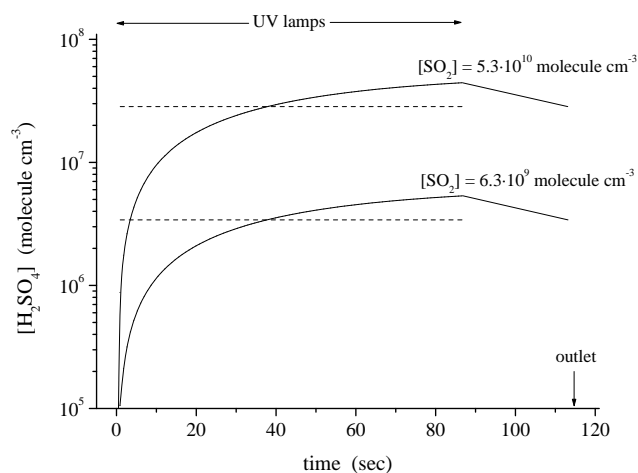
Fig. 1. H$_2$SO$_4$ profiles in the irradiated middle section and the end section of *IfT*-LFT for SO$_2$ concentrations of 6.3×10^9 and 5.3×10^{10} molecule cm^{-3} (total flow: $11\,l\,min^{-1}$ STP; O$_3$: 3.5×10^{11} molecule cm^{-3}; CO: 2.1×10^{14} molecule cm^{-3}). The dashed lines represent the average H$_2$SO$_4$ concentrations in the irradiated middle section of 3.4×10^6 and 2.8×10^7 molecule cm^{-3}.

Fig. 2. Comparison of measured [H$_2$SO$_4$] with modelling results for [H$_2$SO$_4$] for 3 different relative humitities. The dashed line shows the 1:1 line. The total flow in *IfT*-LFT was set at $11\,l\,min^{-1}$ (residence time in irradiated middle section of 88 s). Initial reactant concentrations are (unit: molecule cm^{-3}); O$_3$: 3.4×10^{11}; SO$_2$: $(0.32–23)\times10^{10}$; CO: 2.1×10^{14}.

The dashed lines show the average H$_2$SO$_4$ concentrations in the irradiated middle section, i.e., 3.4×10^6 and 2.8×10^7 molecule cm^{-3} for the considered SO$_2$ concentrations of 6.3×10^9 and 5.3×10^{10} molecule cm^{-3}, respectively. Corresponding maximum H$_2$SO$_4$ concentrations at the end of the irradiated middle section are 5.3×10^6 and 4.4×10^7 molecule cm^{-3}.

3 Results and discussion

3.1 Model evaluation

Experimentally it is difficult to measure H$_2$SO$_4$ concentration directly in the nucleation zone. Loss processes occurring during the transfer of H$_2$SO$_4$ from the nucleation zone to the detector make corrections necessary which represent an additional source of uncertainties. In this study, H$_2$SO$_4$ concentrations are calculated using the measurements of O$_3$ conversion in the irradiated middle section in combination with a kinetic scheme with well-established rate coefficients and well-known concentrations for OH radical consumers (H$_2$, CO, 1,3,5-trimethylbenzene) and SO$_2$.

In order to show the reliability of the modelling for H$_2$SO$_4$ determination the *IfT*-LFT outlet was directly attached to a CI-MS for H$_2$SO$_4$ measurements. Figure 2 shows the comparison of measured H$_2$SO$_4$ concentrations with modelling results for H$_2$SO$_4$ concentrations at the outlet of the *IfT*-LFT for a total gas flow of $11\,l\,min^{-1}$ STP and a relative humidity of 10, 22 or 44%. In the given data the diffusion controlled wall loss in the tubing between *IfT*-LFT outlet and the inlet of the CI-MS has been taken into ac-
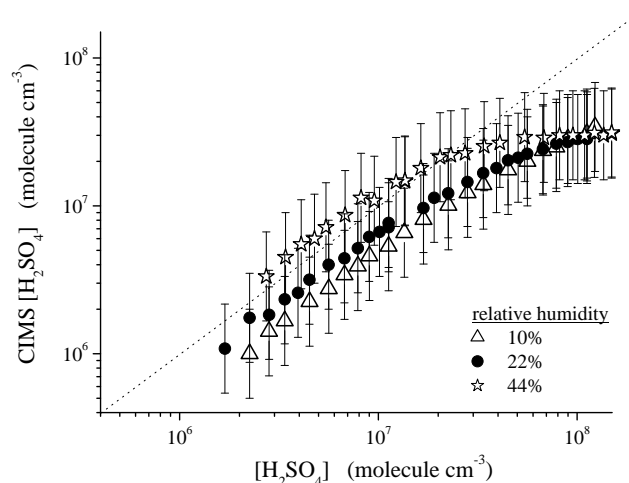
count (length: 97 cm, H$_2$SO$_4$ loss: 41%). Error bars represent the total uncertainty of H$_2$SO$_4$ measurements being approximately a factor of 2. Generally, the modelling results for [H$_2$SO$_4$] are in good agreement with the CI-MS H$_2$SO$_4$ measurements. For relatively high H$_2$SO$_4$ concentrations ([H$_2$SO$_4$] $>(3–5)\times10^7$ molecule cm^{-3}) increasing deviation of measured concentrations from the expected 1:1 line is visible. This behaviour is more pronounced for high RH in the system. Increasing the total gas flow from 11 to $20\,l\,min^{-1}$ STP (i.e. lowering the residence time in the middle and end section from 115 to 62 s) results in less curvature of CI-MS [H$_2$SO$_4$] vs. modelled [H$_2$SO$_4$] in the region of high H$_2$SO$_4$ concentrations, cf. Sipilä et al. (2010). From the kinetic point of view, this behaviour can be explained by additional H$_2$SO$_4$ consuming steps (not accounted for in the model) being more important in the case of high H$_2$SO$_4$ concentrations and long residence times. Initially (for [H$_2$SO$_4$] $>(3–5)\times10^7$ molecule cm^{-3}), the curvature can be described by an additional 2nd order process. With further increasing H$_2$SO$_4$ concentration, the H$_2$SO$_4$-consuming processes gain importance with the overall order being higher than 2. In the same way as the additional loss of H$_2$SO$_4$ out of the gas phase was observed, particle formation became more important with increasing residence time, H$_2$SO$_4$ concentrations and RH, see explanations later. Size distribution measurements revealed that the detected particles (assuming that they consist of H$_2$SO$_4$ exclusively) account only partly for the missing H$_2$SO$_4$ fraction. E.g., at a relative humidity of 44% (simulated [H$_2$SO$_4$] $=1.5\times10^8$ molecule cm^{-3} and CI-MS: [H$_2$SO$_4$] $=3.1\times10^7$ molecule cm^{-3}, cf. Fig. 2) particulate H$_2$SO$_4$ amounts to 2.6×10^7 molecule cm^{-3}. Although
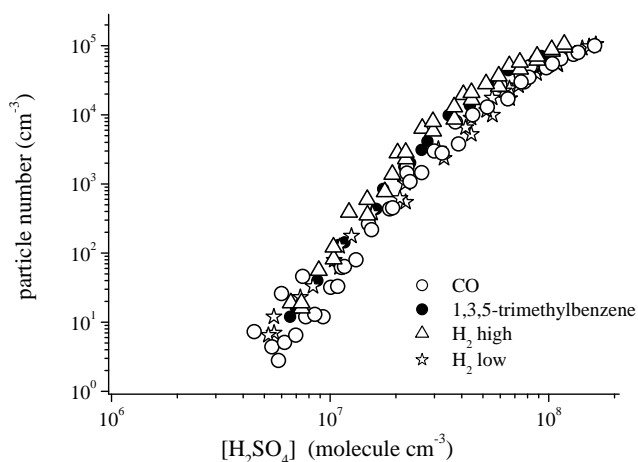
Fig. 3. Total particle numbers for different additives for adjusting OH levels in the flow tube; total gas flow: 3.33 litre min^{-1}; RH = 22%; H$_2$O-based UCPC (TSI 3786), growth tube: 78 °C, saturator: 1 °C. Initial reactant concentrations are (unit: molecule cm^{-3}); O$_3$: $(1.4-3.7) \times 10^{11}$; SO$_2$: $(0.33-806) \times 10^{10}$; CO: 2.1×10^{14}; 1,3,5-trimethylbenzene: 8.4×10^{11}; H$_2$: 1.77×10^{15} or 2.4×10^{17}. The amount of reacted 1,3,5-trimethylbenzene was $(5.6 - 6.4) \times 10^{10}$ molecule cm^{-3}.

Fig. 4. Apparent nucleation rate as a function of H$_2$SO$_4$ concentration for different residence times in the irradiated middle section of the *IfT*-LFT; RH = 22%; butanol-based UCPC (TSI 3025).

uncertainties of the measurements and the model output do not allow a precise mass balance, this indicates that beside the detected particles also H$_2$SO$_4$ containing clusters are present accounting for a significant fraction of missing H$_2$SO$_4$.

3.2 Adjustment of OH concentrations by H$_2$, CO or 1,3,5-trimethylbenzene and the purity of the carrier gas

The predominant fraction of generated OH radicals (via pathway R1) is consumed by H$_2$, CO or 1,3,5-trimethylbenzene in order to lower the OH radical concentration in the flow tube close to atmospheric levels. In each case, the concentrations of the additives are high enough that consumption of OH radicals by diffusion controlled wall loss can be neglected in the modelling scheme, i.e. for example: $k_{R2a}[H_2] \gg k_{wall,OH}$. In Fig. 3 measured particle numbers are depicted from experiments at RH = 22% with a total gas flow of 3.33 l min^{-1} STP using the 3 different additives. Maximum OH concentrations are 2×10^7 ([CO] = 2.1×10^{14}), 8×10^6 ([1,3,5-trimethylbenzene] = 8.4×10^{11}), 4×10^5 ([H$_2$] = 2.4×10^{17}) and 3×10^7 ([H$_2$] = 1.77×10^{15}), all concentrations in molecule cm^{-3}. The particle measurements do not show any dependence on the chemical nature and the concentration of the additive used. This indicates that the additives themselves or reaction products of those are not significantly involved in the nucleation process. In the case of 1,3,5-trimethylbenzene, the disappearance of this organic was followed by means of a GC-FID con-
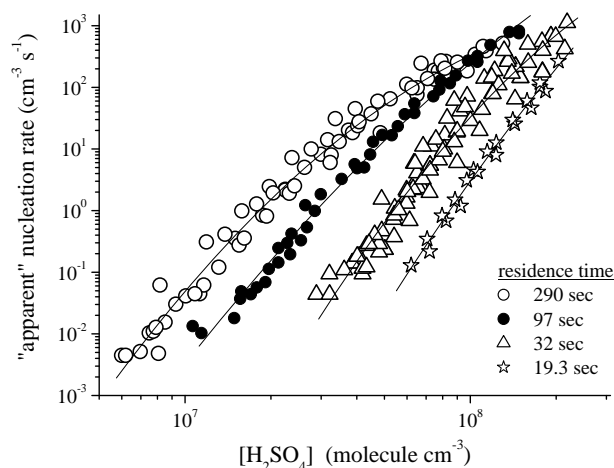
nected with a cryo-enrichment technique. The obtained ratio of reacted 1,3,5-trimethylbenzene and O$_3$, Δ[1,3,5-trimethylbenzene]/Δ[O$_3$] = 2±0.4, supports the validity of the reaction scheme, cf. Sect. 2.3. It is to be noted, that a change of the OH concentration from 4×10^5 molecule cm^{-3} to 3×10^7 molecule cm^{-3} does not influence the number of particles detected. That indicates that also oxidation products arising from any gas impurities (with nearly stable background concentrations) do not significantly contribute to the particle formation observed, as an increase of the OH concentration by about 2 orders of magnitude causes also an up to 2 orders of magnitude higher formation rate of the oxidation products from these impurities. (Note: In each case the detected particle number was a function of H$_2$SO$_4$. If the OH radical concentration was reduced, SO$_2$ had to be increased accordingly.)

The carrier gas used after purification had a stated residual amount of impurities of $< 1.2 \times 10^{10}$ molecule cm^{-3} (NMHCs, H$_2$O and CO$_2$ in sum). By means of on-line GC-FID technique including cryo-enrichment (calibrations using 1,3,5-trimethylbenzene and furan yielded a detection limit of a few 10^9 molecule cm^{-3} for organics) no signals for organic impurities were observed. PTR-MS measurements (Hansel et al., 1998) in the range of 50-250 Dalton have been performed using the pure carrier gas as well as in the presence of H$_2$O and the trace gases. Also as the result of this analysis, there was no indication for the occurrence of any impurities pointing at impurity concentrations below 10^9 molecule cm^{-3} (see Sipilä et al., 2010). However, it is not possible to rule out any impurities being out of range of detectable substances for the analytical techniques applied here.

3.3 Importance of residence time in nucleation experiments

The experimentally observed curves for particle number vs. [H$_2$SO$_4$] measured by means of a butanol-based UCPC (TSI 3025) showed a strong dependence on the residence time of the reaction gas in the flow tube. Scaling by time, i.e. dividing measured particle numbers by the residence time in the irradiated middle section, reveals that also the curves for nucleation rate vs. [H$_2$SO$_4$] are clearly dependent on the residence time, see measurements at RH = 22% in Fig. 4. (The nucleation rate in Fig. 4 is stated as "apparent", for explanation see below.) The measured particle numbers represent the overall result of i) the nucleation process itself, ii) the growth of stable nuclei towards the size detectable with the particle counter used, and iii) the counting efficiency depending on the final particle size. From the data given in Fig. 4 it is obvious that the growth process (coupled with the size-dependent counting efficiency of the counter) governs the particle number measured. The deduced values for J increase with increasing residence time in the flow tube, e.g. for [H$_2$SO$_4$] = 6×10^7 molecule cm^{-3} J rises from 0.1 cm^{-3} s^{-1} (19.3 s) to 100 cm^{-3} s^{-1} (290 s). Consequently, the resulting nucleation rates represent only "apparent" values for J being clearly influenced by the growth process and the ability of the used counter to detect small particles. Measurements of the particle size distribution for a residence time of 290 s and H$_2$SO$_4$ concentrations of ∼10^8 molecule cm^{-3} showed mean particle diameters of ∼3 nm. That is the stated cut-off size of the used butanol-based UCPC (TSI 3025). In this range of H$_2$SO$_4$ concentration the total particle numbers arising from integrating over the size distributions were in reasonable agreement with the numbers of integral measurements. This fact suggests that for these experimental conditions (long residence time and relatively high concentrations of H$_2$SO$_4$ for effective growth) the majority of newly formed particles are measurable by means of the UCPC (TSI 3025) used, and consequently, the resulting nucleation rates J are less affected by particle growth and decreasing counting efficiency.

In a second set of experiments at RH = 22%, particle measurements have been performed by means of a PHA-UCPC and a M-CPC (both counters with a cut-off size down to 1.5 nm in mobility diameter) instead of the butanol-based UCPC (TSI 3025) as used before, cf. Fig. 5. Using these high sensitivity counters no clear dependence of derived nucleation rates on the residence time in the flow tube was observed. Obviously, in this case, particle growth is not the limiting step and the counting efficiency is high enough that the majority of formed particles can be detected. A comparative study using PHA-UCPC, M-CPC and the butanol-based UCPC (TSI 3025) is given by Sipilä et al. (2010). A rough estimate regarding the particle loss in the *IfT*-LFT was carried out assuming a loss process starting in the middle of the irradiated section to the point of detection. For the 3 flow rates
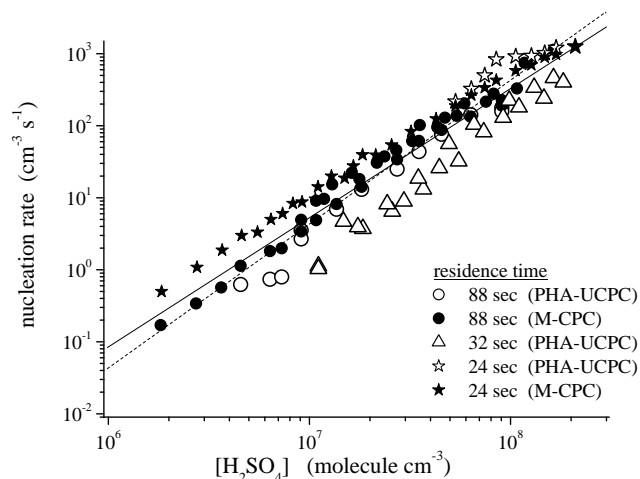

Fig. 5. Nucleation rate as a function of H$_2$SO$_4$ concentration for different residence times in the irradiated middle section of the *IfT*-LFT; RH = 22%. Measurements have been performed by means of PHA-UCPC and M-CPC. Full line represents the overall best fit according to Eq. (1), dashed line stands for the fitting result constraining the exponent for H$_2$SO$_4$ at 2.

used, the loss of 1.5 nm particles amounts to 31% (11 l min^{-1} STP), 13% (30 l min^{-1} STP), or 10% (40 l min^{-1} STP). For larger particles the losses are of less importance. Corrections for particle loss have not been included. Linear regression analysis has been performed according to:

$$\log(J/\text{cm}^{-3}\,\text{s}^{-1}) = \qquad\qquad (1)$$
$$\log(k/\text{cm}^{-3}\,\text{s}^{-1}) + \alpha\log([\text{H}_2\text{SO}_4]/\text{molecule cm}^{-3})$$

(J = nucleation rate). The application of a power equation according to Eq. (1) (here in logarithmic form) is in line with the nucleation theorem (Kashchiev, 1982). In this context, the parameter α stands for the number of H$_2$SO$_4$ molecules in the critical cluster. The analysis yielded α = 1.80±0.06 and k = 1.3×10^{-12} cm^{-3} s^{-1} (full line in Fig. 5). Setting α = 2 as a fixed value, k = 4.2×10^{-14} cm^{-3} s^{-1} follows (dashed line in Fig. 5). For the individual data series in Fig. 5, α is in the range of 1.7–2.1. Constraining α to an integer value, i.e. α = 1 or 2, a number of one or two H$_2$SO$_4$ molecules in the critical cluster follows assuming that the nucleation step is rate limiting. The presence of one or two H$_2$SO$_4$ molecules in the critical cluster is in clear contradiction to the reported values from former laboratory studies, i.e. 4–30 (Wyslouzil et al., 1991), 21 or 10 (Viisanen et al., 1997), 7–13 (Ball et al., 1999), 3–8 (Young et al., 2008), 9–10 (Benson et al., 2009) but in line with Sipilä et al. (2010) using also particle measurements by means of PHA-UCPC and M-CPC. The agreement of α-values from this study with those reported from observations in the atmosphere (Weber et al., 1996; Kulmala et al., 2006; Sihto et al., 2006; Riipinen et al., 2007; Kuang et al., 2008) is
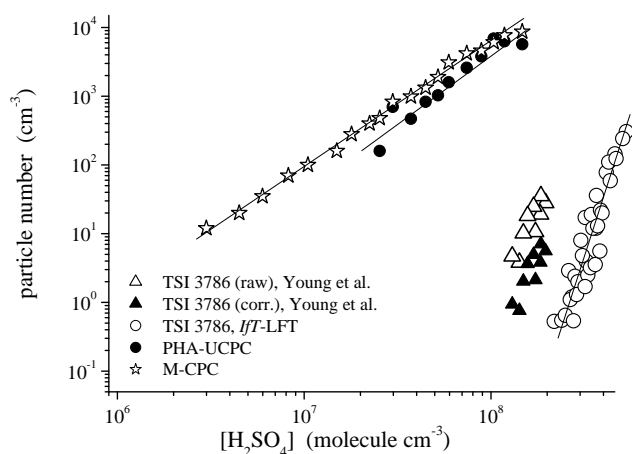
Fig. 6. Measured particle numbers as a function of end-[H$_2$SO$_4$] at 288 K (cf. Figs. 9 and 10 in Young et al., 2008) and as a function of average-[H$_2$SO$_4$] at 293 K from this study (*IfT*-LFT); RH = 15%. Measurements have been done by means of H$_2$O-based UCPC (TSI 3786), PHA-UCPC and M-CPC. UCPC (TSI 3786) used in the *IfT*-LFT experiments operated at the default temperature settings, time for number averaging: 60–300 s. The residence time was 19 s in the Young et al. (2008) experiments. The *IfT*-LFT was operated with a residence time of 19.3 s in the irradiated middle section (25.2 s for middle + end section). For explanation of the corrections done by Young et al. (2008) see the original work.

very good. Kuang et al. (2008) reported pre-exponential K-values according to $J = K$ [H$_2$SO$_4$]^2 from different measurement sites being in the range of $(1–1600) \times 10^{-14}$ cm^3 s^{-1}. The value from this study, $k = 4.2 \times 10^{-14}$ cm^{-3} s^{-1} for $\alpha = 2$ according to Eq. (1), is at the lower end of the range derived from atmospheric measurements. (Note, the different units for K and k arise from the logarithmic notation in Eq. (1), the numerical values are comparable.) Differences in the pre-exponential factors can be probably explained by different H$_2$O concentrations and temperatures during the nucleation events as well as by the occurrence of elevated concentrations of bases (NH$_3$ or amines) at the different sites, see later.

3.4 Comparison of *IfT*-LFT results with nucleation data by Young et al. (2008)

As a case study, results from nucleation experiments by Young et al. (2008) are compared with our findings from the *IfT*-LFT at nearly comparable, experimental conditions. Young et al. (2008) conducted nucleation experiments starting also from OH + SO$_2$ in a flow reactor using Chemical Ionisation Mass Spectrometry (CI-MS) measurements for the determination of H$_2$SO$_4$ concentrations. OH radicals are formed by UV-photolysis of H$_2$O directly at the beginning of the nucleation zone. Figure 6 shows measured particle numbers as a function of end [H$_2$SO$_4$] at 288 K by Young et al. (2008) and the comparable data from *IfT*-LFT as a function of [H$_2$SO$_4$] at 293 K. In both studies the relative humid-

ity was set to 15%. Young et al. (2008) used a residence time of 19 s. In our experiment the residence time in the irradiated middle section was 19.3 s and 25.2 s in total for the middle and end section together. The same kind of particle counter (TSI 3786) was used in both experiments.

When comparing the results by the TSI 3786 counter for a particular concentration of [H$_2$SO$_4$] (e.g. 2×10^8 molecule cm^{-3}) a difference in the integral particle numbers of 2–3 orders of magnitude between our measurements and the results of Young et al. (2008) is observed, cf. Fig. 6. This relatively large difference is mainly caused by the fact that the particle concentration is a steep function of [H$_2$SO$_4$]. Trying to explain the differences in terms of the H$_2$SO$_4$ concentrations, a difference of about a factor of 2 follows. Our H$_2$SO$_4$ concentration represents an average value for the irradiated middle section of the *IfT*-LFT. On the other hand, data given by Young et al. (2008) represent the end H$_2$SO$_4$ concentrations at the system outlet (the initial value is 2.4 times the end value). Furthermore, the axial H$_2$SO$_4$ profiles in both tubes are not identical due to the different approaches applied for H$_2$SO$_4$ production (point source for H$_2$SO$_4$ in the experiment by Young et al. (2008) and continuous H$_2$SO$_4$ formation in the *IfT*-LFT). The different temperatures used in the two experiments, 288 K or 293K, can also influence the results. Generally, higher particle numbers are expected for lower temperatures. In conclusion, when considering the different definitions of H$_2$SO$_4$ concentrations, the different concentration profiles in the flow reactors, and the differences in temperature, it can be stated that results from the two experiments agree within their uncertainties applying the same kind of a particle counter (TSI 3786).

But, comparing the results of integral particle measurements done by the H$_2$O-based TSI 3786 counter with the PHA-UCPC and the M-CPC a clear disagreement is observed regarding both, the threshold H$_2$SO$_4$ concentrations needed for nucleation, and the slopes, $\Delta\log(N)/\Delta\log([H_2SO_4]) = 7.9$ (TSI 3786); 2.0 (PHA-UCPC); 1.8 (M-CPC), cf. also Sipilä et al. (2010). For the short residence time used here as well as for the relatively dry conditions only a small fraction of nucleated particles is able to grow into the detection window of the TSI 3786 counter. This leads to a clear overestimation of the threshold H$_2$SO$_4$ concentrations as well as too steep slopes $\Delta\log(N)/\Delta\log([H_2SO_4])$.

3.5 Influence of H$_2$O vapour

3.5.1 Nucleation rate

In the next set of experiments, particle measurements by means of the PHA-UCPC and the M-CPC were repeated for RH higher than the standard value of 22%, trying to explore the importance of H$_2$O vapour concentration in the process of new particle formation. As a result of a former study using
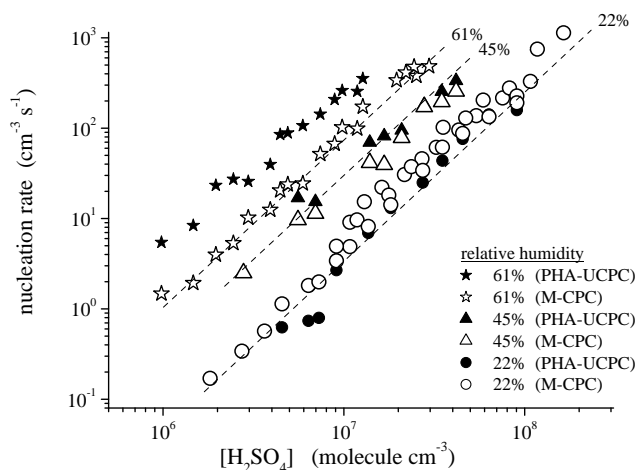
Fig. 7. Nucleation rate as a function of H_2SO_4 concentration for different RH; total gas flow $11\,l\,min^{-1}$ STP. Measurements have been performed by means of PHA-UCPC and M-CPC. The dashed lines stand for the overall best fit according to Eq. (2a), $\alpha = 1.86$ (H_2SO_4), $\beta = 3.08$ (H_2O).

our experimental approach (Berndt et al., 2005), a distinct increase of the particle number with increasing RH was observed. In the present paper, focus was on data for RH > 20% being the most relevant humidities for atmospheric conditions. Figure 7 shows experimental results of the nucleation rate as a function of H_2SO_4 concentrations for a total flow of $11\,l\,min^{-1}$ and 3 different relative humidities. Nucleation rates were obtained by dividing measured particle numbers by the residence time in the irradiated middle section of 88 s. By means of both counters a clear increase of nucleation rate with increasing RH is visible. The results from the PHA-UCPC suggesting stronger RH dependence compared to the M-CPC data. Currently, no explanation for this different behaviour can be given.

For simultaneous determination of the exponent for H_2SO_4 (α) and for RH or H_2O vapour (β) in Eq. (2a) and (2b) all measured data were used.

$$J = k([H_2SO_4]/\text{molecule cm}^{-3})^\alpha (\text{RH}/\%)^\beta \quad (2a)$$

In order to convert the values for RH at 293 K to absolute H_2O vapour concentrations a saturation vapour pressure of 23.41 mbar was applied (Goff, 1946).

$$J = \quad (2b)$$
$$k'([H_2SO_4]/\text{molecule cm}^{-3})^\alpha ([H_2O]/10^{15}\,\text{molecule cm}^{-3})^\beta$$

For carrying out maximum Likelihood estimates of α, β, and k (k') a damped Gauss-Newton technique was applied (Nowak and Deuflhard, 1985). In this least-squares method relative variances were minimised instead of absolute vari-

ances, because the numerical values of derived nucleation rates J span several orders of magnitude.

$$\sum_i (J_i^{\text{model}}/J_i^{\text{measured}} - 1)^2 = \min \quad (3)$$

This approach ensures that relatively small values in the least-square sum are not undervalued.

According to Eq. (2a) the parameter fitting yielded $\alpha = 1.86 \pm 0.03$, $\beta = 3.08 \pm 0.09$ and $k = (2.33 \pm 1.87) \times 10^{-17}$ $cm^{-3}\,s^{-1}$. For Eq. (2b) $\alpha = 1.86 \pm 0.03$, $\beta = 3.08 \pm 0.09$ and $k' = (1.05 \pm 0.98) \times 10^{-19}$ $cm^{-3}\,s^{-1}$ follows. The dashed lines in Fig. 7 show the modelling results using Eq. (2a). Note, α values of 1.6–2.0 were obtained for the individual measurement series by means of linear regression analysis according to Eq. (1). There was no hint that with increasing RH the α values were systematically lowered. Consequently, activation of impurities (potentially arising from e.g. the water saturator) by H_2SO_4 should be of minor importance as such a mechanism should be 1st order in H_2SO_4. Furthermore, it is obvious that the data measured by the PHA-UCPC at RH = 61% are not adequately described using Eq. (2a) or (2b). On the other hand, excluding this data set in the fitting procedure does not change the fitting results significantly (Eq. 2b: $\alpha = 1.88 \pm 0.03$, $\beta = 3.00 \pm 0.08$ and $k' = (1.03 \pm 0.84) \times 10^{-19}$ $cm^{-3}\,s^{-1}$). The exponent $\alpha = 1.86$ for H_2SO_4 is nearly the same as found according to Eq. (1) for the data set at RH = 22% given here and by Sipilä et al. (2010). The exponent for H_2O vapour, $\beta = 3.08$, points at a strong promoting effect of H_2O vapour for nucleation.

It is to be noted here that the analysis of the measured growth rate points to the possible presence of growth-enhancing substances arising e.g. from the water saturator (see section below). Consequently, it cannot be ruled out that also the nucleation was influenced by these impurities, and the exponent $\beta = 3.08$ found for the water dependence must be considered as an upper limit.

Analysis of atmospheric nucleation, however, shows an inhibiting overall effect of H_2O vapour on the nucleation process (Laaksonen et al., 2008), probably caused by any other, indirect effects governing the overall influence of H_2O vapour . From all other laboratory experiments, also an enhancing effect of H_2O vapour is reported. The deduced number of H_2O in the critical cluster (corresponding to β) span a wide range of values, i.e. ~9 (Wyslouzil et al., 1991), 4–6 (Ball et al., 1999), 6–15 (Benson et al., 2009).

Regardless of the fact that β represents an upper limit, simulated nucleation rates according to Eq. (2a) for RH = 22% and RH = 61% have been compared with atmospheric nucleation rates as observed in Heidelberg (February–April 2004) and Hyytiälä (April–May 2005) (Riipinen et al., 2007), cf. Fig. 8. The agreement between simulation and atmospheric observations is good. For comparison, Figure 8 shows also results of parameterizations derived from atmospheric measurements in Tecamac (March 2006) and Hyytiälä (March 2003) as given by Kuang et al. (2008) which are well in line
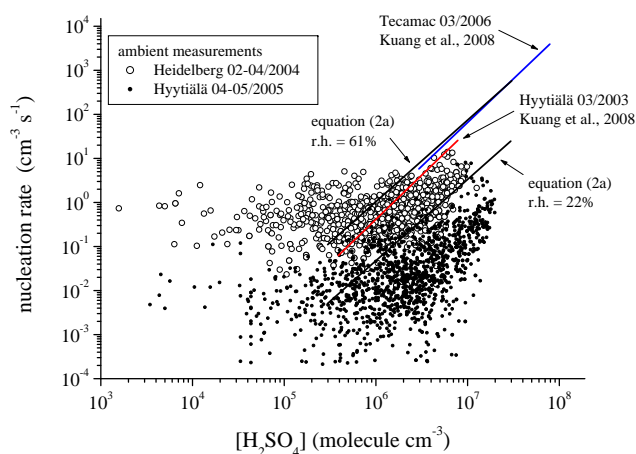
Fig. 8. Comparison of simulated nucleation rates according to Eq. (2a) for RH = 22% and RH = 61% with atmospheric data obtained in Heidelberg and Hyytiälä (Riipinen et al., 2007) as well as results of derived parameterizations from atmospheric measurements in Tecamac and Hyytiälä as given by Kuang et al. (2008). Period of measurements is given behind the sites, month/year.

with Eq. (2a) at least for RH = 61%. The parameterization given here is based on experimental data obtained at 293 K. Atmospheric measurements, however, have been performed in the range of lower temperatures with no definite specification. Lowering of the temperature should cause an increase of the effective rate coefficient k in Eq. (2a). On the other hand, at lower temperatures the H_2O vapour concentration in the atmosphere can drop significantly leading to a decrease of the H_2O term in Eqs. (2a) and (2b). Therefore, a more detailed analysis of atmospheric data considering the influence of RH (H_2O vapour concentration), temperature and background aerosol concentrations and temperature-dependent measurements from the laboratory are needed.

The experimental findings given are clearly contrary to the predictions of the binary homogeneous nucleation theory, H_2SO_4-H_2O (Vehkamäki et al., 2002; Yu, 2007). On the other hand, the laboratory data (except for the water vapour dependence) are well in line with atmospheric measurements of new particle formation events, cf. Fig. 8. It is still unclear what the nucleation mechanism behind our laboratory observations as well as behind the nucleation process in the atmosphere is. We cannot rule out the presence of any impurities in the flow tube with concentrations below a few 10^9 molecule cm^{-3} and, consequently, the participation of a third component (e.g. an amine, see later) in the nucleation process. Obviously, if these impurities are important, they must be present in both the atmosphere and the *IfT*-LFT carrier gas in comparable amounts.
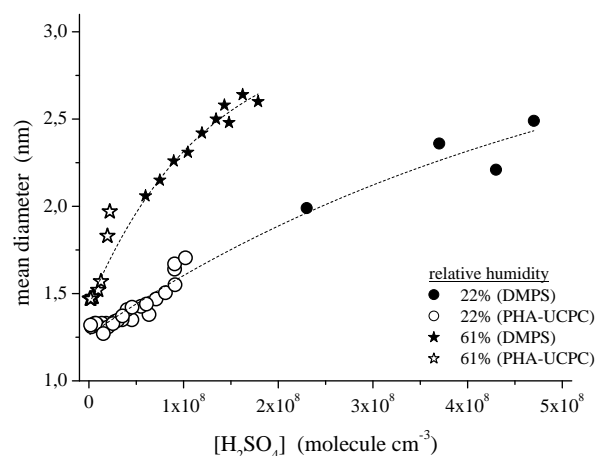

Fig. 9. Detected mean particle diameters from DMPS and PHA-UCPC measurements as a function of H_2SO_4 concentration; RH 22% or 61%; total gas flow 11 l min^{-1} STP.

3.5.2 Particle growth

As a result of PHA-UCPC analysis an increase of the mean particle diameter with increasing RH was visible, i.e. beside the nucleation rate also the growth process is significantly enhanced by H_2O vapour. In Fig. 9 the PHA-UCPC data along with results from DMPS measurements for elevated H_2SO_4 concentrations are depicted. Qualitatively, mean particle diameters derived by both techniques show a similar trend. It is to be noted that diameters of ∼2 nm derived from DMPS measurements can be influenced by the inaccuracy of the CPC counting efficiency applied in the inversion algorithm.

The observed particle growth at RH = 22% is in good agreement with theoretical predictions. The strong enhancement of growth with increasing humidity, however, surpasses the prediction from theoretical considerations (Nieminen et al., 2010). According to this theoretical work, the experimentally observed enhancement of growth is more than expected assuming collision limited growth by H_2SO_4 together with a few co-condensing water molecules per H_2SO_4 molecule. Obviously, water alone is not enough to explain the growth behavior found. The explanation for this strong enhancement is unclear and we cannot exclude the possibility that additional condensing vapors were introduced into the flow tube together with the humidified gas.

3.6 Addition of bases

3.6.1 NH₃

In experiments with NH₃ addition the measurements of NH₃ concentrations have been performed at the inlet and the outlet of *IfT*-LFT by means of an OMNISENS TGA310 system (stated detection limit: 2.5×10^9 molecule cm^{-3}). All measurements shown here were conducted with a total gas flow
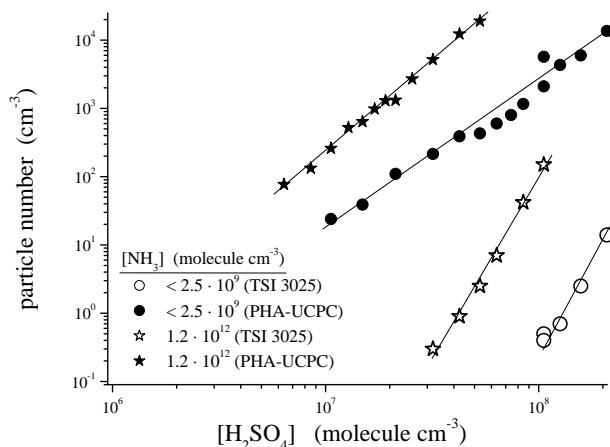
Fig. 10a. Particle numbers as a function of H$_2$SO$_4$ concentration in absence and presence of NH$_3$ addition; total gas flow: $301\,\mathrm{min}^{-1}$ STP. Relative humidity: 13%.
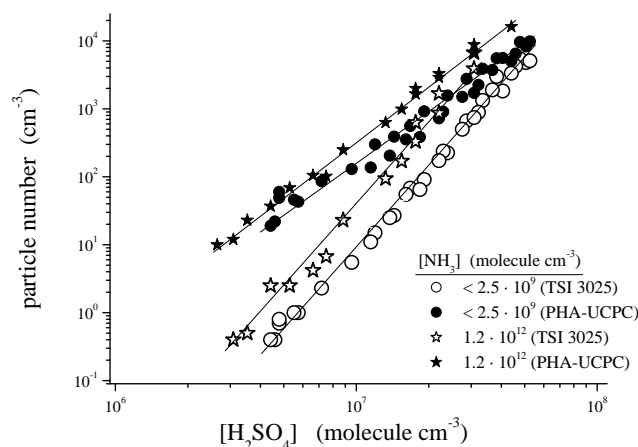

Fig. 10b. Particle numbers as a function of H$_2$SO$_4$ concentration in absence and presence of NH$_3$ addition; total gas flow: $301\,\mathrm{min}^{-1}$ STP. Relative humidity: 47%.

of $301\,\mathrm{min}^{-1}$ STP resulting in a relatively short residence time in the flow tube, 32 sec in the irradiated middle section. Under this flow condition, after a waiting time of about 1 h (to equilibrate gas and walls) the measured NH$_3$ concentrations at the inlet and the outlet were nearly identical. Distinct differences between inlet- and outlet-concentrations were observed in the case of flow rates of $101\,\mathrm{min}^{-1}$ STP and below. Before starting an experiment (without NH$_3$ additions) no NH$_3$ background signal was measureable. For maintenance (avoidance of NH$_3$ memory effects), beside the standard procedure between the experiments and at night-time (flushing with a small stream of dry carrier gas) the flow tube was also flushed under low pressure (10–20 mbar) from time to time and the jacket-temperature was set at 50 °C.

Figure 10a and b show measurements of the particle number as a function of H$_2$SO$_4$ concentrations in absence and presence of a NH$_3$ addition of 1.2×10^{12} molecule cm^{-3} for a relative humidity of 13% and 47%, respectively. A NH$_3$ concentration of 1.2×10^{12} molecule cm^{-3} is representative for a maximum value in agricultural areas (Robarge et al., 2002). In the case of the highly populated area of New York, a mean NH$_3$ mixing ratio of 5 ppbv (1.2×10^{11} molecule cm^{-3}) is reported (Bari et al., 2003). Both NH$_3$ data represent peak concentrations in the atmosphere.

A comparison of the measured particle numbers in Fig.10a and Fig. 10b without NH$_3$ addition shows that in the case of dry conditions (Fig. 10a, RH = 13%; relatively small particles) TSI 3025 is able to detect only a small fraction of the particles counted by PHA-UCPC. For relatively wet conditions (Fig. 10b, RH = 47%; relatively large particles) the measurement series from both counters are closer together and start to merge for high H$_2$SO$_4$ concentrations. Also here it is clearly seen that the counting efficiency of the chosen counter strongly influences the results, cf. explanations in the sections before. Adding 1.2×10^{12} molecule cm^{-3} NH$_3$

an increase of the particle number becomes visible for both counters. The rise of particle number is more pronounced in the case of dry conditions, i.e. 1–2 orders of magnitude at RH = 13% (Fig.10a) and only a factor of 2–5 at RH = 47% (Fig. 10b). Qualitatively these findings are in line with experimental results by Benson et al. (2009) stating that in the case of NH$_3$ addition (5×10^{11} molecule cm^{-3}) the nucleation enhancing effect is distinctly higher for relatively dry conditions, i.e. enhancement by a factor of 1000 at RH = 4% and by a factor of $\sim$2 at RH = 33%. Benson et al. (2009) also concluded that the deduced number of H$_2$SO$_4$ in the critical cluster is lowered in the presence of NH$_3$ indicating a stabilizing effect of the critical cluster. Our measurements did not show a clear change of the slope $\Delta\log(N)/\Delta\log([\mathrm{H_2SO_4}])$ as a result of NH$_3$ addition with exception of PHA-UCPC measurements at RH = 13% suggesting a small rise of the slope. Benson et al. (2009) used in their study a butanol-based TSI 3776 counter. It can be speculated that insufficient counting efficiency of the commercial counter (TSI 3776) affected again the derived slopes $\Delta\log(N)/\Delta\log([\mathrm{H_2SO_4}])$ as given by Benson et al. (2009).

The latest development of ternary H$_2$SO$_4$-NH$_3$-H$_2$O nucleation theory considering the effect of NH$_4$HSO$_4$ formation (Anttila et al., 2005, Merikanto et al., 2007) shows that even for NH$_3$ mixing ratios of 1–10 ppbv (2.4 - 24×10^{10} molecule cm^{-3}) NH$_3$ is not able to influence nucleation at 295 K unless the H$_2$SO$_4$ concentration amounts to at least 10^9 molecule cm^{-3}. That means that state-of-the-art ternary nucleation is not able to describe our findings. Basically, the theory does not allow any ternary nucleation in our system. On the other hand, the classical ternary H$_2$SO$_4$-NH$_3$-H$_2$O nucleation theory (Napari et al., 2002) clearly overestimates the measured new particle formation under our experimental conditions.

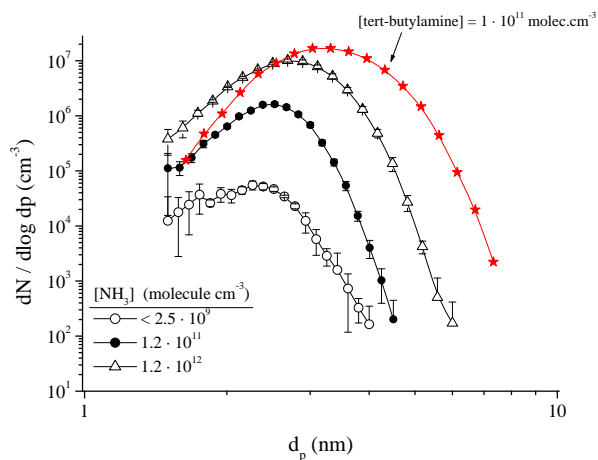**Fig. 11a.** Particle size distributions obtained in absence or presence (1.2×10^{11} or 1.2×10^{12} molecule cm^{-3}) of NH$_3$ additions or tert-butylamine (1.0×10^{11} molecule cm^{-3}); total gas flow: 30 l min^{-1} STP. Relative humidity: 13%; [H$_2$SO$_4$] = 8×10^8 molecule cm^{-3}.

Fig. 11b. Particle size distributions obtained in absence or presence (1.2×10^{11} or 1.2×10^{12} molecule cm^{-3}) of NH$_3$ additions or tert-butylamine (1.5×10^{11} or 7.5×10^{11} molecule cm^{-3}); total gas flow: 30 l min^{-1} STP. Relative humidity: 47%; [H$_2$SO$_4$] = 2×10^8 molecule cm^{-3}.

In Fig. 11a and b size distribution measurements in absence and presence of NH$_3$ additions (1.2×10^{11} or 1.2×10^{12} molecule cm^{-3}) at RH = 13% or 47%, respectively, are given (measurements in the presence of tert-butylamine will be discussed later). It is obvious that NH$_3$ addition leads to a signal increase for all sizes shifting the whole size distribution to higher mean diameters. As expected from the integral measurement (cf. Fig. 10a and b) the NH$_3$ effect appears to be much stronger in the case of low RH. Total particle numbers arising from integration over the size distributions increase in the series 1.1×10^4, 2.7×10^5, 2.1×10^6 cm^{-3} (RH = 13%) and 4.4×10^4, 7.6×10^4, 2.9×10^5 cm^{-3} (RH = 47%) for NH$_3$ additions of 0, 1.2×10^{11} and 1.2×10^{12} molecule cm^{-3}, respectively. The data with NH$_3$ additions given in Fig. 11a and b point at small values for $\Delta\log(N)/\Delta\log([\text{NH}_3])$ being below or close to 1. This finding suggests that the critical clusters stabilized by NH$_3$ can consist of 1 molecule of NH$_3$ and 2 molecules of H$_2$SO$_4$ (for constant NH$_3$ addition: $\Delta\log(N)/\Delta\log([\text{H}_2\text{SO}_4]) \sim 2$). Hanson and Eisele (2002) favoured a critical cluster consisting of 1 molecule of NH$_3$ and 2 molecules of H$_2$SO$_4$ as a result of their cluster measurements in presence of NH$_3$ at 285 K. Benson et al. (2009) concluded that less than 2 NH$_3$ molecules are present in the critical cluster.

NH$_3$, the most abundant base in atmosphere shows a nucleation enhancing effect for relatively high concentrations close to atmospheric peak concentrations. From chemistry point view, acid-base interactions should cause this behaviour. It is not clear why the NH$_3$ effect is much more pronounced in the case of dry conditions. Probably, there is a competition of H$_2$O vapour (or any H$_2$O clusters) and NH$_3$ in the process of critical cluster stabilization. But this scenario is highly speculative at the moment and much more
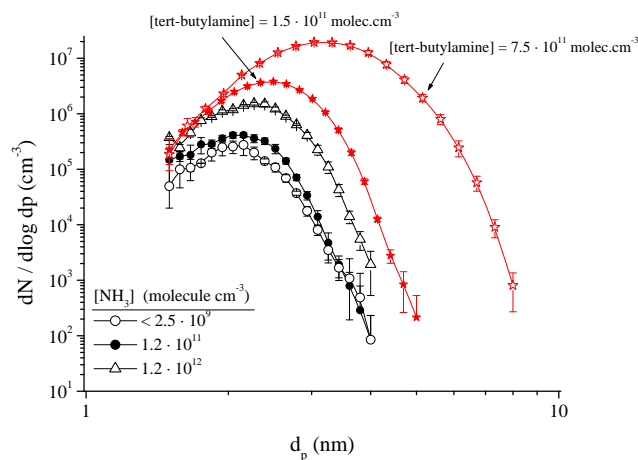
experimental work is needed. Especially from cluster measurements, more insight in the elementary steps determining the process of nucleation is necessary.

3.6.2 Tert-butylamine

Tert-butylamine represents an example of an arbitrary, primary amine. Amines are mainly released into the atmosphere by microbial conversion of organic material as well as by industrial chemistry (Schade and Crutzen, 1995), they are not produced in the course of atmospheric gas-phase oxidation of any organic precursors. There are only a limited number of atmospheric amine measurements available in literature. Sellegri et al. (2003) reported trimethylamine concentrations in the order of 10^9 molecule cm^{-3} measured at the boreal forest site in Hyytiälä. Atmospheric concentrations in the range (0.1–1.8)×10^9 molecule cm^{-3} have been measured at different sites in Sweden for methylamine, dimethylamine, trimethylamine and diethylamine in total at what the lower levels arise from samplings during precipitation (Grönberg et al., 1992). From a measurement site close to a dairy farm, very high concentrations in the order of 10^{12} molecule cm^{-3} have been obtained for a couple of amines as butylamine, diethylamine and pyridine (Rabaud et al., 2003).

Beside the NH$_3$ data, in Fig. 11a and Fig. 11b the nucleation enhancing effect by tert-butylamine is demonstrated for relatively high amine concentrations in the order of 10^{11} molecule cm^{-3} being representative for areas with intensive stock farming. It is to be noted that the given amine concentrations in the experiments are the theoretical (maximum) values after dilution of a gas mixture of tert-butylamine with carrier gas at the *IfT*-LFT entrance assuming no wall losses. The addition of tert-butylamine has a
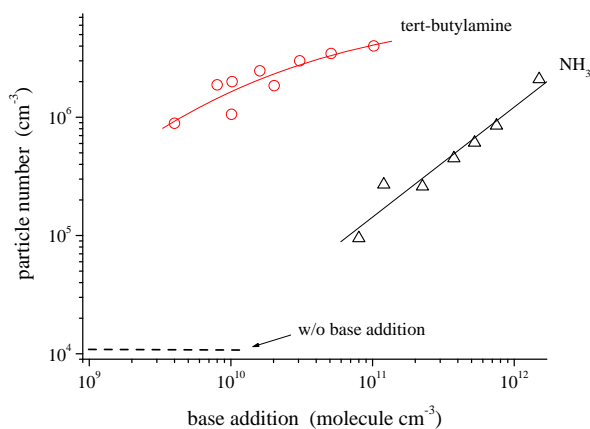
Fig. 12. Total particle numbers by integration of size distributions as a function of base additions (NH$_3$ or tert-butylamine); total gas flow: 30 l min^{-1} STP; Relative humidity: 13%; [H$_2$SO$_4$] = 8×10^8 molecule cm^{-3}.

much stronger effect on nucleation and growth than that of NH$_3$. This behaviour is qualitatively in line with the predictions of quantum chemical methods given by Kurten et al. (2008). The enhancing effects of bases (NH$_3$ and tert-butylamine) in the nucleation process are compared in Fig. 12 showing particle numbers as derived from size distribution measurements as function of base addition at RH = 13%. While in the case of NH$_3$ a linear behaviour can be seen, $\Delta \log(N)/\Delta \log([NH_3]) = 0.93$, for tert-butylamine a curved shape (suggesting a saturation behaviour for higher amine addition) was found with $\Delta \log(N)/\Delta \log([amine])$ being clearly smaller compared to that of NH$_3$. On the absolute scale, however, tert-butylamine addition of about 10^{10} molecule cm^{-3} results in an enhancement of produced particle number by about two orders of magnitude. Extrapolation of the NH$_3$ data down to about 10^{10} molecule cm^{-3} suggests a small or negligible effect of NH$_3$ on nucleation in this concentration range. The compared to NH$_3$ stronger effect observed for tert-butylamine (or maybe amines in general) can be attributed to the enhanced gas-phase basicity (proton affinity) of amines amplifying the acid-base interactions.

These data represent a first experimental observation from laboratory regarding the possible role of amines for atmospheric nucleation and point to a significant nucleation-enhancing effect of amines at least at sites being close to local sources. Mäkelä et al. (2001) observed in the boreal forest that nucleation events were strongly connected to the occurrence of dimethylammonium ions in the particle phase. That indicates that dimethylamine was taking part in the nucleation process and/or the subsequent growth. Recently, the importance of amines for particle growth was emphasized by Smith et al. (2010). These atmospheric observations support the possible role of amines for nucleation and particle growth.

It is to be noted here again that our gas-phase analysis does not allow an ensured detection of carrier gas impurities (including amines) with concentrations below 10^9 molecule cm^{-3}, cf. Sect. 3.2. The strong effect on nucleation observed for tert-butylamine addition of about 10^{10} molecule cm^{-3} reveals that the measurements without defined amine addition could be influenced by amine background traces below 10^9 molecule cm^{-3} being below the detection limit of the gas-phase measurements. If, in our experiment, these background amines are involved in the nucleation process they could also play an important role in atmospheric H$_2$SO$_4$-H$_2$O nucleation, because measurements show that atmospheric amine concentrations can reach 10^8–10^9 molecule cm^{-3} (Grönberg et al., 1992; Sellegri et al., 2003) and definitely higher values close to local sources. Therefore, we consider amines as promising candidates for explaining the existing discrepancies between binary nucleation theory and observations in laboratory and field.

4 Summary

Nucleation experiments starting from the reaction of OH radicals with SO$_2$ have been performed in the *IfT*-LFT flow tube under atmospheric conditions at 293±0.5 K for a relative humidity of 13–61%. The agreement between measured and modelled H$_2$SO$_4$ concentrations at the *IfT*-LFT outlet for commonly used conditions was found to be good suggesting that modelling is able to describe the H$_2$SO$_4$ concentrations in the reaction zone. The addition of H$_2$, CO or 1,3,5-trimethylbenzene for adjusting the OH radical concentration in the flow tube did not influence the nucleation process. Resulting OH radical concentrations were in the range of (4–300)×10^5 molecule cm^{-3}.

The detected number of newly formed particles was found to be strongly dependent on the growth time and the detection efficiency of the particle counter used. High efficiency counters allowed detection of particles with diameters down to about 1.5 nm. The parameterization of measured particle numbers and derived nucleation rates was carried out using power law equations for H$_2$SO$_4$ and for H$_2$O vapour. For measurements at RH = 22% and different residence times the exponent for H$_2$SO$_4$ was in the range of 1.7–2.1. The overall best fit results in a H$_2$SO$_4$ exponent $\alpha = 1.80\pm0.06$. RH-dependent measurements in the range of 22–61% showed a promoting effect of H$_2$O vapour for both the nucleation rate and particle growth. The derived exponent for H$_2$O, $\beta = 3.08$, is regarded as an upper limit.

A comparison of modelling results with ambient measurements in Heidelberg and Hyytiälä (Riipinen et al., 2007) and parameterizations derived from atmospheric measurements in Tecamac and Hyytiälä as given by Kuang et al. (2008) shows that the given parameterisation is able to describe new particle formation as observed in the atmosphere. The impact of atmospherically relevant bases, NH$_3$ and the

sample amine tert-butylamine, was investigated using atmospheric peak concentrations for these substances. Addition of 1.2×10^{11} or 1.2×10^{12} molecule cm^{-3} of NH$_3$ (NH$_3$ background $< 2.5 \times 10^9$ molecule cm^{-3}) revealed that NH$_3$ has a promoting effect on both the nucleation rate and particle growth. The enhancing effect was found to be more pronounced for relatively dry conditions, i.e. 1–2 orders of magnitude in nucleation rate at RH = 13% and a factor of 2–5 at RH = 47% ([NH$_3$] = 1.2×10^{12} molecule cm^{-3}). Explaining this behaviour, it can be speculated that probably there is a competition of H$_2$O vapour (or any H$_2$O clusters) and NH$_3$ in the process of critical cluster stabilization. Adding tert-butylamine (as an arbitrary sample amine) instead of NH$_3$, the enhancing effect for nucleation and particle growth was found to be much stronger. Measurements at RH = 13% with a tert-butylamine addition of about 10^{10} molecule cm^{-3} show an enhancement of produced particles by about two orders of magnitude, whereas extrapolation of the NH$_3$ data down to concentrations of about 10^{10} molecule cm^{-3} suggests only a small or negligible effect of NH$_3$. This strong effect indicates that the measurements without a definite amine addition could be influenced by any amine background traces below 10^9 molecule cm^{-3} being below the detection limit of our gas-phase measurements. If these possible background amines are significantly involved in the nucleation process they can also play an important role in atmospheric H$_2$SO$_4$-H$_2$O nucleation because atmospheric measurements show amine concentrations in the range 10^8–10^9 molecule cm^{-3} (Grönberg et al., 1992; Sellegri et al., 2003) and definitely higher values close to local sources. Therefore, amines are probably promising candidates explaining existing discrepancies between binary nucleation theory and observations.

Edited by: M. Gysel

References

Anttila, T., Vehkamäki, H., Napari, I., and Kulmala, M.: Effect of ammonium bisulfate formation on atmospheric water-sulfuric acid-ammonia nucleation, Boreal Environ. Res., 10, 511–523, 2005.

Ball, S. M., Hanson, D. R., Eisele, F. L., and McMurry, P. H.: Laboratory studies of particle nucleation: Initial results for H$_2$SO$_4$, H$_2$O, and NH$_3$ vapors, J. Geophys. Res., 104, 23709–23718, doi:10.1029/1999JD900411, 1999.

Baria, A., Ferraro, V., Wilson, L. R., Luttinger, D., and Husain, L.: Measurements of gaseous HONO, HNO$_3$, SO$_2$, HCl, NH$_3$, particulate sulfate and PM$_{2.5}$ in New York, NY, Atmos. Environ., 37, 2825–2835, 2003.

Benson, D. R., Erupe, M. E., and Lee, S.-H.: Laboratory-measured H$_2$SO$_4$-H$_2$O-NH$_3$ ternary homogeneous nucleation rates: Initial observations, Geophys. Res. Lett., 36, L15818, doi:10.1029/2009GL038728, 2009.

Berndt, T., Böge, O., Stratmann, F., Heintzenberg, J., and Kulmala, M.: Rapid Formation of Sulfuric Acid Particles at Near-Atmospheric Conditions, Science, 307, 698–700, 2005.

Berndt, T., Stratmann, F., Bräsel, S., Heintzenberg, J., Laaksonen, A., and Kulmala, M. : SO$_2$ oxidation products other than H$_2$SO$_4$ as a trigger of new particle formation. Part 1: Laboratory investigations, Atmos. Chem. Phys., 8, 6365–6374, doi:10.5194/acp-8-6365-2008, 2008.

Coffman, D. J. and Hegg, D. A.: A preliminary study of the effect of ammonia on particle nucleation in the boundary layer, J. Geophys. Res., 100, 7147–7160, 1995.

DeMore, W. B., Sander, S. P., Golden, D. M., Hampson, R. F., et al.: Chemical kinetics and photochemical data for use in stratospheric modelling. Evaluation number 12, JPL Publication 97-4, 1–266, 1997.

Dick, W. D., McMurry, P. H., Weber, R. J., and Quant, R.: White-light Detection for Nanoparticle sizing with the TSI ultrafine condensation particle counter, J. Nanoparticle Res., 2, 85–90, 2000.

Eisele, F. L. and Tanner, D.: Measurement of the gas phase concentration of H$_2$SO$_4$ and methane sulfonic acid and estimates of H$_2$SO$_4$ production and loss in the atmosphere, J. Geophys. Res., 98, 9001–9010, 1993.

Friend, J. P., Barnes, R. A., and Vasta, R. M.: Nucleation by Free Radicals from the Photooxidation of Sulfur Dioxide in Air, J. Phys. Chem., 84, 2423–2438, 1980.

Goff, J. A.: Saturation pressure of water on the new Kelvin temperature scale, Transactions of the American Society of Heating and Ventilating Engineers. Technical report, presented at the semi-annual meeting of the American Society of Heating and Ventilating Engineers, Murray Bay, Quebec Canada, 347–354, 1957.

Grönberg, L., Lövkvist, P., and Jönsson, J. A.: Measurement of Aliphatic Amines in Ambient Air and Rainwater, Chemosphere, 24, 1533–1540, 1992.

Hansel, A., Jordan, A., Warnike, C., Holzinger, R., and Lindinger, W.: Improved detection limit of the proton-transfer reaction mass spectrometer: On-line monitoring of volatile organic compounds at mixing ratios of a few PPTV: Rapid. Commun. Mass Spectrom., 12, 871–875, 1998.

Hanson, D. R. and Eisele, F. L.: Diffusion of H$_2$SO$_4$ in humidified nitrogen: Hydrated H$_2$SO$_4$, J. Phys. Chem. A, 104, 1715–1719, 2000.

Hanson, D. R. and Eisele, F. L.: Measurement of prenucleation molecular clusters in the NH$_3$, H$_2$SO$_4$, H$_2$O system, J. Geophys. Res., 107, D124158, doi:10.1029/2001JD001100, 2002.

Iida, K., Stolzenburg, M. R., and McMurry, P. H.: Effect of Working Fluid on Sub-2 nm Particle Detection with a Laminar Flow Ultrafine Condensation Particle Counter, Aerosol Sci. Technol., 43(1), 81–96, 2009.

Kashchiev, D.: On the relation between nucleation work, nucleus size and nucleation rate, J. Chem. Phys., 76, 5098–5102, 1982.

Korhonen, P. M., Kulmala, M., Laaksonen, A., Viisanen, Y., McGraw, R., and Seinfeld, J. H.: Ternary nucleation of H$_2$SO$_4$, NH$_3$, and H$_2$O in the atmosphere, J. Geophys. Res., 104, 26349–26353, 1999.

Kramp, F, and Paulson, S. E.: On the uncertainties in the rate coefficients for OH reactions with hydrocarbons, and the rate coefficients of the 1,3,5-trimethylbenzene and m-xylene reactions with OH radicals in the gas phase, J. Phys. Chem. A, 102, 2685–2690, 1998.

Kuang C., McMurry, P. H., McCormick, A. V., and Eisele, F. L.: Dependence of nucleation rates on sulfuric acid vapor concentration in diverse atmospheric locations, J. Geophys. Res., 113, D10209, doi:10.1029/2007JD009253, 2008.

Kulmala, M., Laaksonen, A., and Pirjola, L.: Parameterization for sulphuric acid/water nucleation rates, J. Geophys. Res., 103, 8301–8307, 1998.

Kulmala, M., K. E. J. Lehtinen, and A. Laaksonen: Cluster activation theory as an explanation of the linear dependence between formation rate of 3 nm particles and sulphuric acid concentration, Atmos. Chem. Phys., 6, 787–793, doi:10.5194/acp-6-787-2006, 2006.

Kurten, T., Loukonen, V., Vehkamäki, H., and Kulmala, M.: Amines are likely to enhance neutral and ion-induced sulfuric acid-water nucleation in the atmosphere more efficiently than ammonia, Atmos. Chem. Phys., 8, 4095–4103, doi:10.5194/acp-8-4095-2008, 2008.

Laaksonen, A., Kulmala, M., Berndt, T., Stratmann, F., Mikkonen, S., Ruuskanen, A., Lehtinen, K. E. J., Dal Maso, M., Aalto, P., Petäjä, T., Riipinen, I., Sihto, S.-L., Janson, R., Arnold, F., Hanke, M., Ücker, J., Umann, B., Sellegri, K., O'Dowd, C. D., and Viisanen, Y.: SO$_2$ oxidation products other than H$_2$SO$_4$ as a trigger of new particle formation. Part 2: Comparison of ambient and laboratory measurements, and atmospheric implications, Atmos. Chem. Phys., 8, 7255-7264, doi:10.5194/acp-8-7255-2008, 2008.

Mauldin III, R. L., Frost, G., Chen, G., Tanner, D., Prévôt, A., Davis, D., and Eisele, F.: OH measurements during the First Aerosol Characterization Experiment (ACE 1): Observations and model comparisons, J. Geophys. Res., 103, 16713–16729, 1998.

Mauldin, III, R. L., Eisele, F., Tanner, D., Kosciuch, E., Shetter, R., Lefer, B., Hall, S. R., Nowak, J. B., Buhr, M., Chen, G., Wang, P., and Davis, D.: Measurements of OH, H$_2$SO$_4$, and MSA at the South Pole during ISCAT, Geophys. Res. Lett., 28, 3629–3632, 2001.

Mäkelä, J. M., S. Yli-Koivisto, V. Hiltunen, W. Seidl, E. Swietlicki, K. Teinilä, M. Sillanpää, I. K. Koponen, J. Paatero, K. Rosman, and K. Hämeri: Chemical composition of aerosol during particle formation events in boreal forest, Tellus, 53B, 380–393, 2001.

McMurry, P. H. and Friedlander, S. K.: New Particle Formation in the Presence of an Aerosol, Atmos. Environ, 13, 1635–1651, 1979.

Merikanto, J., Napari, I., Vehkamäki, H., Anttila, T., and Kulmala, M.: New parameterization of sulphuric acid-ammonia-water ternary nucleation rates at tropospheric conditions, J. Geophys. Res., 112, D15207, doi:10.1029/2006JD007977, 2007.

Napari, I., Noppel, M., Vehkamäki, H., and Kulmala, M.: Parameterization of ternary nucleation rates for H$_2$SO$_4$-NH$_3$-H$_2$O vapors, J. Geophys. Res., 107(D19), 4381, doi:10.1029/2002JD002132, 2002.

Nieminen, T., Lehtinen, K. E. J., and Kulmala, M.: On condensational growth of clusters and nanoparticles in sub-10 nm size range, Atmos. Chem. Phys. Discuss., 10, 1693–1717, doi:10.5194/acpd-10-1693-2010, 2010.

Nowak, U. and Deuflhard, P.: Numerical Identification of Selected Rate Constants in Large Chemical Reaction Systems, Appl. Numer. Math., 1, 59–75, 1985.

Petäjä, T., Mauldin III, R. L., Kosciuch, E., McGrath, J., Nieminen, T., Paasonen, P., Boy, M., Adamov, A., Kotiaho, T., and Kulmala, M.: Sulfuric acid and OH concentrations in a boreal forest site, Atmos. Chem. Phys., 9, 7435–7448, doi:10.5194/acp-9-7435-2009, 2009.

Rabaud, N. E., Ebeler, S. E., Ashbaugh, L. L., and Flocchini, R. G.: Characterization and quantification of odorous and non-odorous volatile organic compounds near a commercial dairy in California, Atmos. Environ., 37, 933–940, 2003.

Riipinen, I., Sihto, S.-L., Kulmala, M., Arnold, F., Dal Maso, M., Birmili, W., Saarnio, K., Teinilä, K., Kerminen, V.-M., Laaksonen, A., and Lehtinen, K. E. J.: Connections between atmospheric sulphuric acid and new particle formation during QUEST IIIIV campaigns in Heidelberg and Hyytil, Atmos. Chem. Phys., 7, 1899–1914, doi:10.5194/acp-7-1899-2007, 2007.

Robarge, W. P., Walker, J. T., McCulloch, R. B., and Murray, G.: Atmospheric concentrations of ammonia and ammonium at an agricultural site in the southeast United States, Atmos. Environ., 36, 1661–1674, 2002.

Schade, G. W. and Crutzen, P. J.: Emission of Aliphatic Amines from Animal Husbandry and their Reactions: Potential Source of N$_2$O and HCN, J. Atmos. Chem., 22, 319–346, 1995.

Sellegri, K., M. Hankel, B. Umann, F. Arnold, and M. Kulmala: Measurement of organic gases during aerosol formation events in the boreal forest atmosphere during QUEST, Atmos. Chem. Phys., 5, 373–384, doi:10.5194/acp-5-373-2005, 2005.

Sgro, L. A. and Fernández de la Mora, J.: A simple turbulent mixing CNC for charged particle detection down to 1.2 nm, Aerosol Sci. Technol., 38, 1–11, 2004.

Sihto, S.-L., Kulmala, M., Kerminen, V.-M., Dal Maso, M., Petäjä, T., Riipinen, I., Korhonen, H., Arnold, F., Janson, R., Boy, M., Laaksonen, A., and Lehtinen, K. E. J.: Atmospheric sulphuric acid and aerosol formation: implications from atmospheric measurements for nucleation and early growth mechanisms, Atmos. Chem. Phys., 6, 4079–4091, doi:10.5194/acp-6-4079-2006, 2006.

Sipilä, M., Lehtipalo, K., Kulmala, M., Petäjä, T., Junninen, H., Aalto, P. P., Manninen, H. E., Kyrö, E.-M., Asmi, E., Riipinen, I., Curtius, J., Kürten, A., Borrmann, S., and O'Dowd, C. D.: Applicability of condensation particle counters to measure atmospheric clusters, Atmos. Chem. Phys., 8, 4049–4060, doi:10.5194/acp-8-4049-2008, 2008.

Sipilä, M., Lehtipalo, K., Attoui, M., Neitola, K., Petäjä, T., Aalto, P. P., O'Dowd, C. D., and Kulmala, M.: Laboratory verification of PH-CPC's ability to monitor atmospheric sub-3 nm clusters, Aerosol Sci. Technol., 43, 126-135, 2009.

Sipilä, M., Berndt, T., Petäjä, T., Brus, D., Vanhanen, J., Stratmann, F., Petakoski, J., Mauldin, L., Hyvärinen, A.-P., Lihavainen, H., and Kulmala, M.: The Role of Sulphuric Acid in Atmospheric Nucleation, Science, 327, 1243–1246, 2010.

Smith, J. N., Barsanti, K. C., Friedl, H. R., Ehn, M., Kulmala, M., Collins, D. R., Scheckman, J. H., Williams, B. J., and McMurry, P. H.: Observations of aminium salts in atmospheric nanoparticles and possible climatic implications, P.N.A.S., 107, 6634–6639, 2010.

Stockwell, W. R. and Calvert, J. G.: The mechanism of the HO-SO$_2$ reaction, Atmos. Environ., 17, 2231–2235, 1983.

Stratmann, F. and Wiedensohler, A.: A new data inversion algorithm for DMPS-measurements, J. Aerosol Sci., 27, 339–340, 1996.

Vehkamäki, H., Kulmala, M., Napari, I., Lehtinen, K. E. J., Timmreck, C., Noppel, M., and Laaksonen, A.: An improved parameterization for sulfuric acid – water nucleation rates for tropospheric and stratospheric conditions, J. Geophys. Res., 107(D22), 4622, doi:10.1029/2002JD002184, 2002.

Vanhanen, J.: Mixing-type CPC detecting charged clusters down to 1.05 nm, presented at ICNAA 2009, Prague, 2009.

Viisanen, Y., Kulmala, M., and Laaksonen, A.: Experiments on gasliquid nucleation of sulphuric acid and water, J. Chem. Phys., 107, 920–926, 1997.

Weber, R. J., McMurry, P. H., Eisele, F. L., and Tanner, D. J.: Measurement of expected nucleation precursor species and 3-500-nm diameter particles at Mauna Loa observatory, Hawaii, J. Atmos. Sci., 52, 2242–2257, 1995.

Weber, R. J., Marti, J. J., McMurry, P. H., Eisele, F. L., Tanner, D. J., and Jefferson, A.: Measured atmospheric new particle formation rates: Implications for nucleation mechanisms, Chem. Eng. Comm., 151, 53–64, 1996.

Wyslouzil, B. E., Seinfeld, J. H., Flagan, R. C., and Okuyama, K.: Binary nucleation in acid-water systems. II. Sulphuric acid-water and a comparison with methanesulphonic acid-water, J. Chem. Phys., 94, 6842–6850, 1991.

Young, L.-H., D. R. Benson, F. R. Kameel, J. R. Pierce, H. Junninen, M. Kulmala, and S.-H. Lee: Laboratory studies of H$_2$SO$_4$/H$_2$O binary homogeneous nucleation from the SO$_2$+OH reaction: Evaluation of the experimental setup and preliminary results, Atmos. Chem. Phys., 8, 4997–5016, doi:10.5194/acp-8-4997-2008, 2008.

Yu, F.: Improved quasi-unary nucleation model for binary H$_2$SO$_4$ – H$_2$O homogeneous nucleation, J. Chem. Phys., 127, 05401, 2007.

Zellner, R: Recombination reactions in atmospheric chemistry, Ber. Bunsenges. Phys. Chem., 82, 1172–1179, 1978.

Zhang, R., Suh, I., Zhao, J., Zhang, D., Fortner, E. C., Tie, X., Molina, L. T., and Molina, M. J.: Atmospheric New Particle Formation Enhanced by Organic Acids, Science, 304, 1487–1489, 2004.